Comparison of the optical properties of pre-colored dental monolithic zirconia ceramics sintered in a conventional furnace versus a microwave oven

Hee-Kyung Kim[1], Sung-Hun Kim[2]*

[1]Department of Dentistry, Ajou University School of Medicine, Suwon, Republic of Korea
[2]Department of Prosthodontics and Dental Research Institute, School of Dentistry, Seoul National University, Seoul, Republic of Korea

PURPOSE. The purpose of this study was to compare the optical properties of pre-colored dental monolithic zirconia ceramics of various thicknesses sintered in a microwave and those in a conventional furnace. **MATERIALS AND METHODS.** A2-shade of pre-colored monolithic zirconia ceramic specimens (22.0 mm × 22.0 mm) in 3 thickness groups of 0.5, 1.0, and 1.5 mm were divided into 2 subgroups according to the sintering methods (n=9): microwave and conventional sintering. A spectrophotometer was used to obtain CIELab color coordinates, and translucency parameters and CIEDE2000 color differences (ΔE_{00}) were measured. The relative amount of monoclinic phase (X_m) was estimated with x-ray diffraction. The surface topography was analyzed by atomic force microscope and scanning electron microscope. Statistical analyses were conducted with two-way ANOVA (α=.05). **RESULTS.** There were small interaction effects on CIE L^*, a^*, and TP between sintering method and thickness ($P<.001$): L^* (partial eta squared η_p^2=0.115), a^* (η_p^2=0.136), and TP (η_p^2=0.206), although higher b^* values were noted for microwave sintering regardless of thickness. Color differences between two sintering methods ranged from 0.52 to 0.96 ΔE_{00} units. The X_m values ranged from 7.03% to 9.89% for conventional sintering, and from 7.31% to 9.17% for microwave sintering. The microwave-sintered specimen demonstrated a smoother surface and a more uniform grain structure compared to the conventionally-sintered specimen. **CONCLUSION.** With reduced processing time, microwave-sintered pre-colored dental monolithic zirconia ceramics can exhibit similar color perception and translucency to those by conventional sintering. *[J Adv Prosthodont 2017;9:394-401]*

KEYWORDS: Y-TZP ceramics; Color; Microwaves; Spectrophotometry

INTRODUCTION

Zirconia-based dental restorations are fabricated using CAD/CAM systems combined with high-temperature sintering. Zirconia ceramics can be processed by either milling a pre-sintered porous blank and subsequent sintering or milling a fully sintered block.[1] For the soft milling of pre-sintered blanks, specific sintering conditions such as sintering temperature and time could influence the mechanical and optical properties of zirconia restorations.[2,3] The hard machining of a fully sintered block requires specifically designed strong milling systems, and the process can therefore induce residual stresses promoting low temperature degradation.[4]

Microwaves have been used in the zirconia processing for over twenty years. In a microwave oven, heat is applied internally as well as externally to the materials, providing rapid heating rates with less thermal stress.[5,6] In addition, the thermal conductivity can be enhanced by using suscep-

Corresponding author:
Sung-Hun Kim
Department of Prosthodontics and Dental Research Institute, School of Dentistry, Seoul National University, Daehakno 101, Jongno-gu, Seoul 03080, Republic of Korea
Tel. +82220722664: e-mail, ksh1250@snu.ac.kr

tors that transform electromagnetic energy into heat.[7] It was reported that microwave sintering had several advantages over conventional sintering, such as reduced time and energy,[7,8] improved densification processes with accelerated grain growth,[9] more uniform surface quality with similar mechanical properties and density,[7,8,10,11] and smaller grain size[12-14] compared to the conventional method.

Pre-colored dental monolithic zirconia ceramics have recently been developed to promote color matching with high mechanical strength and toughness. Due to their improved translucency, pre-colored monolithic zirconia ceramics can be used in the anterior as well as the posterior regions. Various fabrication techniques have been investigated and homogenously-colored zirconia ceramics in different shades are available in the market nowadays.[15]

Most of the studies on the microwave sintering have focused on heat transfer mechanisms and evaluated the physical properties and microstructures. However, the optical properties of microwave-sintered zirconia ceramics have not been extensively studied. Therefore, the purpose of this in vitro study was to compare the optical properties of pre-colored dental monolithic zirconia ceramics of various thicknesses sintered in a microwave and a conventional furnace. In addition, the crystalline phase transformation and the surface topography of pre-shaded monolithic zirconia ceramics obtained by two different sintering methods were evaluated. The null hypotheses were that sintering methods would not affect the optical properties of pre-colored monolithic zirconia ceramics and that the effect of sintering methods on the optical properties of pre-colored monolithic zirconia ceramics would not be affected by the thickness.

MATERIALS AND METHODS

Square-shaped (22.0 mm × 22.0 mm) specimens of three different thicknesses (1.2 mm, 1.7 mm, and 2.3 mm, n = 18 per group) were prepared from a pre-shaded dental monolithic zirconia block (ZrO_2, Y_2O_3 4 - 6%, $HfO_2 \leq 5\%$, $Al_2O_3 \leq 1\%$, Other oxides; lot no. 14I19-03; Rainbow Shade A2, Genoss, Suwon, Korea). Each thickness group was further divided into two subgroups according to the sintering methods: conventional and microwave sintering (n = 9 per subgroup, Table 1). Final thicknesses of each group were then adjusted to 0.5 mm, 1.0 mm, and 1.5 mm by using a horizontal grinding machine (HRG-150, AM Technology, Asan, Korea) and the thicknesses were verified using a digital cali-

per (Digimatic micrometer, Mitutoyo, Tokyo, Japan) with a resolution of 0.01 mm. Before the measurements were performed, all samples were ultrasonically cleaned in isopropyl alcohol for 5 minutes.

Spectral reflectance data from 360 to 750 nm were obtained at 10-nm intervals against a white polytetrafluoroethylene (PTFE) background (GM29010330, X-Rite, Grand Rapids, MI, USA; CIE $L^* = 93.968$, $a^* = -0.168$, and $b^* = 2.476$), a black glass ceramic tile (CM-A101B, Konica Minolta, Tokyo, Japan; CIE $L^* = 0.012$, $a^* = 0.022$, and $b^* = 0.00$), and an A2 glass ceramic tile (IPS e.max Press MO, Ivoclar Vivadent AG, Schaan, Liechtenstein; CIE $L^* = 74.44$, $a^* = -1.95$, and $b^* = 11.462$) with a spectrophotometer (Color iControl, X-Rite, Grand Rapids, MI, USA). Diffuse/8-degree geometry and specular component excluded (de:8°) condition were used for the reflectance measurements. A 6-mm diameter aperture and a 6-mm diameter measurement area were applied. CIELab color coordinates were calculated from the spectral power data relative to D65 with the 2-degree standard colorimetric observer. Five measurements for each specimen were recorded with a medium of distilled water (refractive index of 1.33). Color parameters of an A2 shade tab (classical A1-D4 shade guide, VITA Zahnfabrik, Bad Säckingen, Germany) were also measured and served as a control.

For the calculation of the color differences, averaged color values of each subgroup against an A2 background were used. CIEDE2000 color differences (ΔE_{00}) between two different sintering methods at each thickness and between each subgroup and an A2 shade tab were determined by using the following formula:[16,17]

$$\Delta E_{00} = \left[\left(\frac{\Delta L'}{K_L S_L} \right)^2 + \left(\frac{\Delta C'}{K_C S_C} \right)^2 + \left(\frac{\Delta H'}{K_H S_H} \right)^2 + R_T \left(\frac{\Delta C'}{K_C S_C} \right) \left(\frac{\Delta H'}{K_H S_H} \right) \right]^{\frac{1}{2}}$$

where $\Delta C'$ and $\Delta H'$ are the differences in chroma and hue; S_L, S_C, and S_H are the weighting functions; K_L, K_C, and K_H are the parametric factors; and R_T is a rotation function.[17] The parametric factors were set to 1.[16] The translucency parameters (TP) of each subgroup were calculated from the CIEDE2000 color differences (ΔE_{00}) between the color values of the specimens against a white and a black background.[18]

The crystalline phase analysis was peformed with X-ray diffraction (XRD; D8 ADVANCE, Bruker, Karlsruhe, Germany) using Cu-Kα radiation (λ = 1.5406 Å). One rep-

Table 1. Sintering protocols used in this study

Sintering conditions	Sintering furnace	Total sintering time	Maximum temperature
Conventional	P310 (Nabertherm, Germany)	8 hours	1500°C for 2 hours
Microwave	Sintermat 1600 (Unicera Inc., Korea)	2 hours	1500°C for 30 minutes

resentative specimen per each subgroup was selected and the specimens were scanned from 20 to 40 2θ degrees with a step size of 0.01-degrees and a scan speed of 2-degrees per minute. The monoclinic peak intensity ratio (X_m) and the monoclinic volume content (V_m) on the specimen's surface were calculated with the formulas (A)[19] and (B)[20] below:

(A) $$X_m = \frac{I_m(-111) + I_m(111)}{I_m(-111) + I_m(111) + I_t(101)}$$

(B) $$V_m = \frac{1.311 X_m}{1 + 0.311 X_m}$$

where $I_m(-111)$ and $I_m(111)$ are the monoclinic peak intensities at 2θ = 28.175° and 31.468°, respectively, and $I_t(101)$ is the tetragonal peak intensity at 2θ = 29.807°

The surface topographic analyses at a microscopic level were performed with an atomic force microscope (AFM; XE-100, Park systems, Suwon, Korea) and a scanning electron microscope (SEM; S-4700 SEM, Hitachi High-Technologies Co. Ltd., Tokyo, Japan). For the AFM examination, one representative specimen from each sintering group of 1.5 mm thickness was submitted to the analysis. The images were acquired in the non-contact mode (PPP-NCHR-50 probes, Force constant = 42 N/m) from an area of 10 μm × 10 μm (512 × 512 pixels per image) at a scan rate of 0.20 Hz using a specific software (XEI, XE-100, Park systems, Suwon, Korea). In addition, the average arithmetic mean roughness value (Ra) was obtained.

For the SEM examination, one representative specimen from each sintering group of 1.5 mm thickness was pol-ished and thermally etched for 20 minutes at 1350°C. The specimens were then sputtered with platinum (Q150T Sputter Coater, Quorum Technologies Ltd., Ashford, Kent, UK) and photographs were taken with an accelerating voltage of 15 kV at magnifications of ×10000, ×30000, and ×50000.

Statistical data analyses were conducted by means of SPSS software (v23.0, IBM Corp., Chicago, IL, USA). The Shapiro-Wilk test was used to determine if the dependent variables (CIE L^*, a^*, b^*, and TP) were normally distributed. Two-way ANOVA was performed to determine the effects of two factors (sintering method and thickness) on each continuous outcome variable. The interactions between the two factors were identified and simple main effects of independent variables were analyzed. In addition, the effect sizes and statistical powers were calculated. Statistical significance was set to 0.05 for all analyses.

RESULTS

Means (and standard deviations) for CIE L^*, a^*, and b^* values against an A2 background and TP values of each subgroup and mean color values of an A2 shade tab are listed in Table 2. Two-way ANOVA analysis revealed that there was a statistically significant interaction between the sintering methods and thicknesses on CIE L^* (F (2, 264) = 17.198, P < .001). The interaction effect of sintering method combined with thickness was relatively small for CIE L^* (η_p^2 = 0.115). The statistical power with α = 0.05 was 1.000 (Table 3). Simple main effects analysis showed that L^* val-

Table 2. Means (SD) for CIE L^*, a^*, and b^* values against an A2 background and TP values of each subgroup and mean color values of an A2 shade tab

Sintering/ thickness	L^*	a^*	b^*	TP
Conventional / 0.5	72.15 (.73)	-1.81 (.09)	14.81 (.53)	11.52 (.15)
Conventional / 1.0	69.44 (.87)	-1.37 (.09)	15.41 (.36)	7.87 (.13)
Conventional / 1.5	68.90 (1.05)	-1.20 (.07)	14.33 (.33)	5.31 (.20)
Microwave / 0.5	72.60 (.32)	-1.65 (.09)	15.35 (.50)	11.43 (.15)
Microwave / 1.0	70.36 (.71)	-0.99 (.17)	16.10 (.79)	7.50 (.11)
Microwave / 1.5	68.57 (.34)	-0.93 (.17)	15.07 (.48)	5.28 (.12)
A2 shade tab	60.27 (.01)	-0.20 (.01)	11.95 (.01)	

Table 3. Results of two-way ANOVA with dependent variable CIE L^*

Source of variation	Type III sum of squares	df	Mean square	F	P	Partial Eta Squired	Observed power
Sintering	8.026	1	8.026	15.449	< .001	.055	.975
Thickness	622.227	2	311.114	598.898	< .001	.819	1.000
Sintering × Thickness	17.868	2	8.934	17.198	< .001	.115	1.000
Error	137.142	264	.519				
Total	1336441.990	270					

ues significantly decreased as the thickness increased for conventional (F (2, 264) = 263.466, P < .001) as well as microwave sintering (F (2, 264) = 352.630, P < .001). In addition, higher $L*$ values were noted for microwave sintering compared to conventional sintering at 0.5 mm (F (1, 264) = 8.547, P = 0.004) and 1.0 mm (F (1, 264) = 36.607, P < 0.001), while higher $L*$ value was noted for conventional sintering compared to microwave sintering at 1.5 mm (F (1, 264) = 4.691, P = 0.031) (Table 4).

There was a statistically significant interaction between the sintering methods and thicknesses on CIE $a*$ (F (2, 264) = 20.724, P < .001). The interaction effect of sintering method combined with thickness was relatively small for CIE $a*$ (η_p^2 = 0.136). The statistical power with α = .05 was 1.000 (Table 5). Simple main effects analysis showed that $a*$ values significantly increased as the thickness increased for conventional sintering (F (2, 264) = 308.543, P < .001) as

well as microwave sintering (F (2, 264) = 508.415, P < .001). In addition, higher $a*$ values were noted for microwave sintering compared to conventional sintering at 0.5 mm (F (1, 264) = 37.344, P < .001), 1.0 mm (F (1, 264) = 231.517, P < .001), and 1.5 mm (F (1, 264) = 113.990, P < .001).

No interaction was found between the sintering methods and thicknesses on CIE $b*$ (F (2, 264) = 0.989, P = .373). The statistical power with α = .05 was .221 (Table 6). Independent samples t-Test showed that there was a significant difference in $b*$ values between conventional and microwave sintering (t(268) = 7.906, P < .001, d = 0.96). Higher $b*$ values were noted for microwave sintering.

There was a statistically significant interaction between the sintering methods and thicknesses on TP (F (2, 264) = 34.257, P < .001). The interaction effect of sintering method combined with thickness was relatively small for TP (η_p^2 = 0.206). The statistical power with α = .05 was 1.000

Table 4. Results of pairwise comparisons for simple main effects of sintering methods with dependent variable CIE $L*$

Thickness (mm)		Sum of squares	df	Mean square	F	P
0.5	Contrast	4.440	1	4.440	8.547	.004
	Error	137.142	264	.519		
1.0	Contrast	19.016	1	19.016	36.607	< .001
	Error	137.142	264	.519		
1.5	Contrast	2.437	1	2.437	4.691	.031
	Error	137.142	264	.519		

Table 5. Results of two-way ANOVA with dependent variable CIE $a*$

Source of variation	Type III sum of squares	df	Mean square	F	P	Partial Eta squired	Observed power
Sintering	4.864	1	4.864	341.404	< .001	.564	1.000
Thickness	22.689	2	11.345	796.234	< .001	.858	1.000
Sintering × Thickness	.591	2	.295	20.724	< .001	.136	1.000
Error	3.761	264	.014				
Total	504.415	270					

Table 6. Results of two-way ANOVA with dependent variable CIE $b*$

| Source of variation	Type III sum of squares	df	Mean square	F	P	Partial Eta squired	Observed power
Sintering	28.910	1	28.910	107.121	< .001	.289	1.000
Thickness	52.187	2	26.094	96.685	< .001	.423	1.000
Sintering × Thickness	.534	2	.267	.989	.373	.007	.221
Error	71.249	264	.270				
Total	62352.931	269					

Table 7. Results of two-way ANOVA with dependent variable TP

Source of variation	Type III sum of squares	df	Mean square	F	P	Partial Eta squired	Observed power
Sintering	1.797	1	1.797	84.972	< .001	.243	1.000
Thickness	1747.867	2	873.934	41316.667	< .001	.997	1.000
Sintering × Thickness	1.449	2	.725	34.257	< .001	.206	1.000
Error	5.584	264	.012				
Total	19706.809	270					

(Table 7). Simple main effects analysis showed that TP values significantly decreased as the thickness increased for conventional sintering (F (2, 264) = 20740.663, $P <$ .001) as well as microwave sintering (F (2, 264) = 20610.262, $P <$ .001). In addition, higher TP values were noted for conventional sintering compared to microwave sintering at 0.5 mm (F (1, 264) = 9.474, $P =$ .002) and 1.0 mm (F (1, 264) = 143.160, $P <$ .001). Sintering methods had no effect on TP values at 1.5 mm (F (1, 264) = 0.852, $P =$ .357).

CIEDE2000 color difference (ΔE_{00}) values between the two sintering methods at each thickness were evaluated: 0.52 ΔE_{00} units at 0.5 mm; 0.96 ΔE_{00} units at 1.0 mm; and 0.63 ΔE_{00} units at 1.5 mm. ΔE_{00} values between each subgroup and an A2 shade tab were calculated: 9.97 ΔE_{00} units between conventional /0.5 and an A2 tab; 7.97 ΔE_{00} units between conventional /1.0 and an A2 tab; 7.39 ΔE_{00} units between conventional /1.5 and an A2 tab; 10.32 ΔE_{00} units between microwave /0.5 and an A2 tab; 8.69 ΔE_{00} units between microwave /1.0 and an A2 tab; 7.20 ΔE_{00} units between microwave /1.5 and an A2 tab.

The XRD patterns in the 2θ range from 20 to 40° of each subgroup are shown in Fig. 1. For all subgroups, the XRD analyses revealed similar diffraction patterns. The major peaks of the tetragonal phase were located at 29.807° (2θ), corresponding to the orientation t(101). The peaks of the tetragonal phase were also detected at 33.995° and 34.828° (2θ), corresponding to the t(002) and t(110) crystallographic phases, respectively. For the monoclinic phase, small peaks were observed at 28.175° and 31.468° (2θ), corresponding to m(-111) and m(111) directions. The relative amounts of the monoclinic phase on each specimen are listed in Table 8. The monoclinic peak intensity ratios (X_m) detected on the surfaces of the specimens ranged from 7.03% to 9.89% for conventional sintering, and from 7.31% to 9.17% for microwave sintering. The calculated volume fractions (V_m) of monoclinic phase ranged from 9.02% to 12.58% for conventional sintering, and from 9.37% to 11.69% for microwave sintering. The smallest amounts of monoclinic phase were found on the specimens of 1.0-mm thickness for both sintering methods.
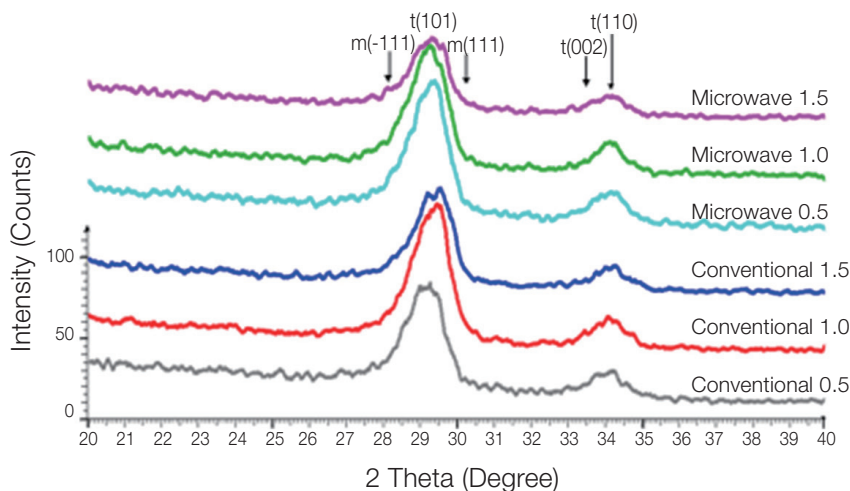

Fig. 1. X-ray diffraction patterns of 6 subgroups at 2θ range between 20 to 40°.

**Table 8.** Relative amount of monoclinic phase verified by X-ray diffractometry

Sintering / thickness	Monoclinic peak intensity ratio (X_m in %)	Monoclinic volume content (V_m in %)
Conventional / 0.5	9.12	11.63
Conventional / 1.0	7.03	9.02
Conventional / 1.5	9.89	12.58
Microwave / 0.5	8.26	10.56
Microwave / 1.0	7.31	9.37
Microwave / 1.5	9.17	11.69

Fig. 2 shows characteristic surface topographic patterns of the conventional- and microwave-sintered specimens (1.5 mm thickness). The AFM images demonstrated the scratch lines induced in the cutting stage to adjust final thicknesses. In addition, the monoclinic spots were detected along the scratches. AFM analyses revealed Ra value of 0.054 µm for the conventionally-sintered specimen and 0.034 µm for the microwave-sintered specimen.

SEM micrographs of the specimens with conventional and microwave sintering are shown in Fig. 3. The microwave-sintered specimen demonstrated a uniform equiaxed grain structure with an average grain size of approximately 250 nm, whereas the conventionally-sintered specimen exhibited a non-uniform grain structure with smaller grains that were approximately 100 - 250 nm in size.
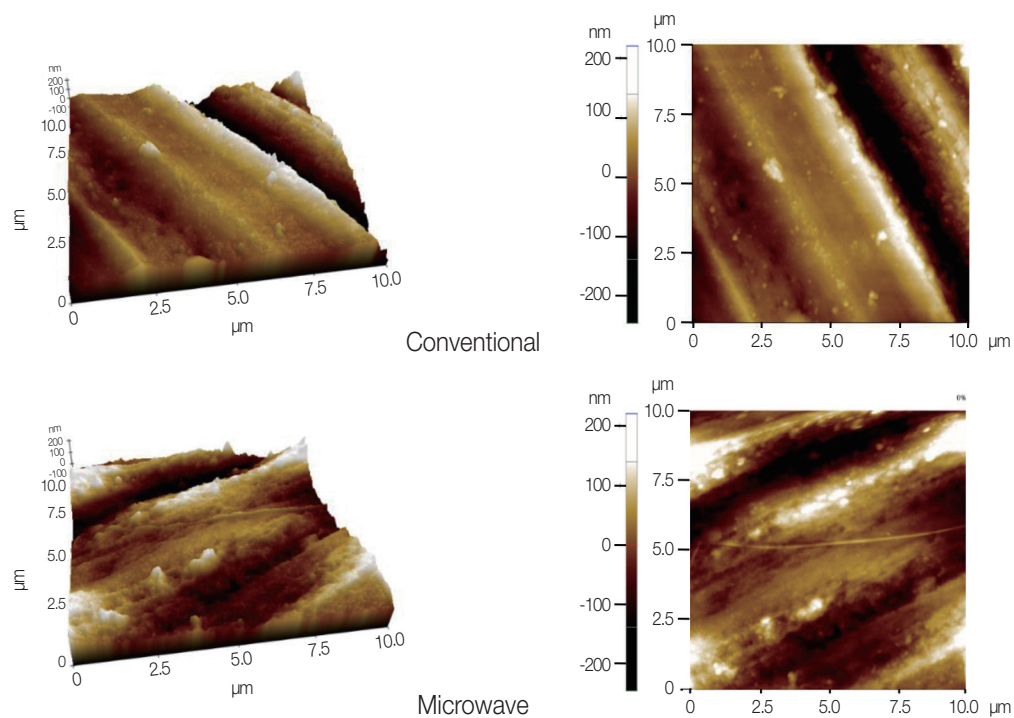
Fig. 2. Atomic force micrographic images (10 µm × 10 µm) of the specimens by using conventional and microwave sintering methods.
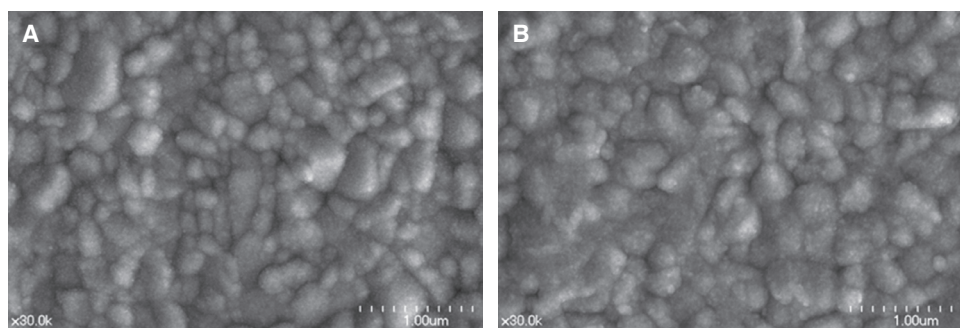
Fig. 3. Scanning electron microscopy images (× 30000) of the specimens (1.5 mm thickness). (A) Specimen by conventional sintering, (B) Specimen by microwave sintering.

DISCUSSION

Based on the results of this study, the null hypotheses were rejected because significant differences in the CIE L^*, a^*, b^*, and TP values were found between sintering methods and the CIE L^*, a^*, and TP values were affected by the thickness. Previous literatures reported that sintering conditions could affect the optical properties of the ceramics.[3,4,21,22] Ebeid et al.[22] found that translucency increased as the sintering time and temperature increased because reduced pores and increased density induced less light scattering with more transmission. Similarly, this study found that the specimens by conventional sintering with longer processing time exhibited higher translucency values. Kim et al.[14] investigated that decreased sintering time led to smaller grains and smaller grains resulted in reduced light scattering and more light transmission. O et al.[23] demonstrated that for the grain smaller than one-third of the wavelength of the light, the transmittance increased in accordance with Rayleigh scattering and the transmittance increased with decreasing grain size. In the present study, microwave sintering produced slightly larger grain size although both sintering processes produced nano-sized grains (approximately 100 - 300 nm) and conventional sintering offered slight increase in translucency. From the SEM views of this study, the grains of microwave sintering had relatively-equiaxial shapes and were arranged in a uniform-packed appearance causing better specular reflection; therefore, higher color values were noted compared to those of conventional sintering ($P < .001$).

The color differences between conventional and microwave sintering were 0.52 ΔE_{00} unit at 0.5 mm, 0.96 ΔE_{00} unit at 1.0 mm, and 0.63 ΔE_{00} unit at 1.5 mm and these color differences could not be detected according to the criteria of 50:50% perceptibility threshold values based on the previous studies.[24-26] The color differences between an A2 shade tab and each subgroup ranged from 7.20 to 10.32 ΔE_{00} units, which could be considered as clinically unacceptable according to the criteria of 50:50% acceptability threshold values based on the previous studies.[24-27] Therefore, the results of this study indicated that pre-colored monolithic zirconia ceramics would not match the corresponding shade guides.

There were small interaction effects on CIE L^*, a^*, and TP between sintering method and thickness ($P < .001$): L^* (partial eta squared $\eta_p^2 = 0.115$), a^* ($\eta_p^2 = 0.136$), and TP ($\eta_p^2 = 0.206$), although higher b^* values were noted for microwave sintering regardless of thickness. Several studied have reported that the optical properties of ceramics could be affected by the thicknesses.[28-30] In this study, as the thickness increased, significant reduction in L^* values and increase in a^* values were observed, while no significant differences in b^* values were recorded regardless of sintering methods, which was comparable to the results of one previous study.[28] The translucency was decreased as the thickness increased for both sintering methods, which was consistent with the results of previous studies.[29,30]

As reported in the previous studies, sintered Y-TZP ceramics had tetragonal and cubic phases without monoclinic phase.[31,32] Hallmann et al.[32] investigated that monoclinic volume fraction (V_m) of Y-TZP abraded with 150-µm alumina particle was 8.68% and roughness value (Ra) was 0.91 µm, while V_m of Y-TZP abraded with 150-µm zirconia particle was 1.22% and Ra, 0.08 µm. In this study, relatively large fractions of monoclinic phase were noted (Xm, 7.03% - 9.89%; Vm, 9.02% - 12.58%) for both sintering methods, which might be attributed to the cutting procedure to adjust final thicknesses. Furthermore, different amounts of monoclinic phase were measured among different thicknesses within the same sintering method. The XRD patterns revealed that doublet configurations were observed at 29.807° (2θ), corresponding to t(101) for the specimens in 1.5-mm thickness of both sintering methods. Any structural changes of lattice parameters depending on the thickness might be expected, and therefore further study should be required. A previous study reported that the thicker specimen displayed more accurate peak appearance.[33]

In the present study, the specimen by microwave sintering had smoother surface (Ra = 0.034 µm) than that by conventional sintering (Ra = 0.054 µm). These results may be due to the grains with uniform size and shape in the microwave-sintered specimen. Therefore, in terms of the optical properties, microwave-sintered pre-colored monolithic zirconia ceramics would exhibit similar color appearance and smoother surfaces with the reduced processing time and cost compared to those sintered in a conventional furnace. The limitations of this study were possible edge loss effect of spectrophotometric reflectance measurements and the use of a limited shade of a specific manufacturer.

CONCLUSION

With reduced processing time, microwave-sintered pre-colored monolithic zirconia ceramics can exhibit similar color perception and translucency to those by conventional sintering.

ORCID

Hee-Kyung Kim *https://orcid.org/0000-0002-9079-6086*
Sung-Hun Kim *https://orcid.org/0000-0003-3289-9703*

REFERENCES

1. Denry I, Kelly JR. State of the art of zirconia for dental applications. Dent Mater 2008;24:299-307.
2. Chevalier J, Deville S, Münch E, Jullian R, Lair F. Critical effect of cubic phase on aging in 3mol% yttria-stabilized zirconia ceramics for hip replacement prosthesis. Biomaterials 2004;25:5539-45.
3. Stawarczyk B, Ozcan M, Hallmann L, Ender A, Mehl A, Hämmerlet CH. The effect of zirconia sintering temperature on flexural strength, grain size, and contrast ratio. Clin Oral Investig 2013;17:269-74.

4. Huang H. Machining characteristics and surface integrity of yttria stabilized tetragonal zirconia in high speed deep grinding. Mater Sci Eng A 2003;345:155-63.

5. Sutton W. Microwave processing of ceramic materials. Am Ceram Soc Bull 1989;68:376-86.

6. Oghbaei M, Miraee O. Microwave versus conventional sintering: A review of fundamentals, advantages and applications. J Alloys Compd 2010;494:175-89.

7. Almazdi AA, Khajah HM, Monaco EA Jr, Kim H. Applying microwave technology to sintering dental zirconia. J Prosthet Dent 2012;108:304-9.

8. Nightingale SA, Worner HK, Dunne DP. Microstructural development during the microwave sintering of yttria-zirconia ceramics. J Am Ceram Soc 1997;80:394-400.

9. Nightingale SA, Dunne DP, Worner HK. Sintering and grain growth of 3 mol% yttria zirconia in a microwave field. J Mater Sci 1996;31:5039-43.

10. Upadhyaya DD, Ghosh A, Dey GK, Prasad R, Suri AK. Microwave sintering of zirconia ceramics. J Mater Sci 2001; 36:4707-10.

11. Denry I, Kelly JR. Emerging ceramic-based materials for dentistry. J Dent Res 2014;93:1235-42.

12. Wilson J, Kunz SM. Microwave sintering of partially stabilized zirconia. J Am Ceram Soc 1988;71:C40-1.

13. Janney MA, Calhoun CL, Kimrey HD. Microwave sintering of solid oxide fuel cell materials: I, zirconia-8 mol% yttria. J Am Ceram Soc 1992;75:341-6.

14. Kim MJ, Ahn JS, Kim JH, Kim HY, Kim WC. Effects of the sintering conditions of dental zirconia ceramics on the grain size and translucency. J Adv Prosthodont 2013;5:161-6.

15. Kim HK, Kim SH. Optical properties of pre-colored dental monolithic zirconia ceramics. J Dent 2016;55:75-81.

16. Commission Internationale de l'Eclairage (CIE). Colorimetry. Technical report CIE publication no. 15:2004, 3rd ed. Vienna, Austria: Central Bureau of the CIE; 2004.

17. Luo MR, Cui G, Rigg B. The development of the CIE 2000 color-difference formula: CIEDE2000. Color Res Appl 2001; 26:340-50.

18. Johnston WM, Ma T, Kienle BH. Translucency parameter of colorants for maxillofacial prostheses. Int J Prosthodont 1995;8:79-86.

19. Garvie RC, Nicholson PS. Phase analysis in zirconia systems. J Am Ceram Soc 1972;55:303-5.

20. Toraya H, Yoshimura M, Somiya S. Calibration curve for quantitative analysis of the monoclinic-tetragonal ZrO2 system by X-ray diffraction. J Am Ceram Soc 1984;67:C119-21.

21. Chen IW, Wang XH. Sintering dense nanocrystalline ceramics without final-stage grain growth. Nature 2000;404:168-71.

22. Ebeid K, Wille S, Hamdy A, Salah T, El-Etreby A, Kern M. Effect of changes in sintering parameters on monolithic translucent zirconia. Dent Mater 2014;30:e419-24.

23. O YT, Koo JB, Hong KJ, Park JS, Shin DC. Effect of grain size on transmittance and mechanical strength of sintered alumina. Mat Sci Eng A 2004;374:191-5.

24. Ghinea R, Pérez MM, Herrera LJ, Rivas MJ, Yebra A, Paravina RD. Color difference thresholds in dental ceramics. J Dent 2010;38:e57-64.

25. Xu BT, Zhang B, Kang Y, Wang YN, Li Q. Applicability of CIELAB/CIEDE2000 formula in visual color assessments of metal ceramic restorations. J Dent 2012;40:e3-9.

26. Paravina RD, Ghinea R, Herrera LJ, Bona AD, Igiel C, Linninger M, Sakai M, Takahashi H, Tashkandi E, Perez Mdel M. Color difference thresholds in dentistry. J Esthet Restor Dent 2015;27:S1-9.

27. Perez MM, Ghinea R, Herrera LJ, Ionescu AM, Pomares H, Pulgar R, Paravina RD. Dental ceramics: a CIEDE2000 acceptability thresholds for lightness, chroma and hue differences. J Dent 2011;39:e37-44.

28. Ozturk O, Uludag B, Usumez A, Sahin V, Celik G. The effect of ceramic thickness and number of firings on the color of two all-ceramic systems. J Prosthet Dent 2008;100:99-106.

29. Sulaiman TA, Abdulmajeed AA, Donovan TE, Ritter AV, Vallittu PK, Närhi TO, Lassila LV. Optical properties and light irradiance of monolithic zirconia at variable thicknesses. Dent Mater 2015;31:1180-7.

30. Kim HK, Kim SH, Lee JB, Han JS, Yeo IS, Ha SR. Effect of the amount of thickness reduction on color and translucency of dental monolithic zirconia ceramics. J Adv Prosthodont 2016;8:37-42.

31. Scott HG. Phase relationships in the zirconia-yttria system. J Mater Sci 1975;10:1527-35.

32. Hallmann L, Ulmer P, Wille S, Polonskyi O, Köbel S, Trottenberg T, Bornholdt S, Haase F, Kersten H, Kern M. Effect of surface treatments on the properties and morphological change of dental zirconia. J Prosthet Dent 2016;115: 341-9.

33. Garvie RC, Nicholson PS. Phase analysis in zirconia systems. J Am Ceram Soc 1972;55:303-5.